Stratigraphic controls on eformation patterns in fault-related folds: a detachment fold example from the Sierra Madre Oriental, northeast Mexico

Mark P. Fischer*, Patricia B. Jackson

Department of Geology and Environmental Geosciences, Northern Illinois University, DeKalb, IL 60115-2854, USA

Abstract

Deformation patterns are described by the style, intensity and distribution of structures throughout a volume of rock. In fault-related folds, presently observed deformation patterns are controlled by structural factors like kinematic history, environmental factors like burial history and stratigraphic factors like layer thickness and competence. To demonstrate the role of stratigraphy in controlling fold-related deformation patterns, we document the stratigraphic variability of mesostructures at one structural position on a map-scale detachment fold. Unique assemblages of faults, fractures and cleavages in certain stratigraphic intervals define a mechanical stratigraphy comprised of several units, each exhibiting a characteristic deformation response to the folding process. The varying response of each mechanical unit suggests that folding mechanisms such as orthogonal flexure, flexural slip or flexural flow, were sequentially or coevally operative in each of the units. Using the simple, theoretical strain distributions associated with each folding mechanism and the fact that each mechanical unit accommodates fold-related strain by developing a characteristic set of mesostructures, we are able to predict general deformation patterns elsewhere in the fold. The significance of this approach is that it recognizes that even in a single structure, fold kinematics and deformation response may be dramatically different in various parts of a stratigraphic section. Because of this, the quality and character of reservoir rocks in anticlinal traps may change markedly over short stratigraphic distances. Predictions of fold-related deformation based solely on fold kinematics are unlikely to resolve these variations. © 1999 Published by Elsevier Science Ltd. All rights reserved.

1. Introduction

The pattern of deformation within a volume of rock is described by the style, intensity and distribution of deformation features throughout that rock volume. The style of deformation characterizes the kinds of deformation features that are present, for example, cleavage, joints, shear fractures, faults and folds. The intensity of deformation describes the degree to which rocks are deformed and can be determined from data such as finite strain, fracture spacing, fault displacements, and fracture apertures (e.g. Ramsay and Huber, 1987a, pp. 107–113; Wojtal, 1989; Gross and

Engelder, 1995; Gross et al., 1997a). The distribution of deformation describes where in the rock volume deformation occurs, as well as the geometries and orientations of deformation features that are present.

At most scales of observation, geologic deformation patterns are controlled by a combination of structural, stratigraphic and environmental factors. This is true for flat-lying rocks in weakly deformed sedimentary basins and strongly deformed rocks in fault-related folds. In the latter case, structural factors influencing deformation patterns are ultimately tied to the kinematic evolution of the fold, because rocks presently in different structural positions on the fold (e.g. the hinge vs the limb) may have undergone unique kinematic histories. These different histories may control fracture and cleavage orientations, overprinting of fabrics and the intensity of fabric development. Stratigraphic fac-

tors influencing deformation patterns include lithology, competence contrasts, strength anisotropy and interface strength. These factors may influence the dominance of brittle vs ductile deformation, the tendency for interbed slip, and the fault slip to propagation ratio (e.g. Tanner, 1989; Fischer and Woodward, 1992; Cooke and Pollard, 1997; Hardy and Ford, 1997). Environmental factors influencing deformation patterns include stress state, temperature and the character of fluids that may have been present during deformation. These factors may control the dominant microscopic deformation mechanisms, the constitutive behavior of the involved materials, or the relative rates of folding and faulting processes (e.g. Jamison, 1992; Lemiszki et al., 1994).

With the advent of rigorous cross-section balancing techniques (Dahlstrom, 1969; Elliott, 1983; Woodward et al., 1985), the significance of deformation patterns in fault-related folds has been realized from both theoretical and applied perspectives. Numerous workers in the last decade have recorded deformation patterns in natural fault-related folds and used these patterns to reconstruct fold kinematics (e.g. Mitchell and Woodward, 1988; Fischer et al., 1992; Rowan and Kligfield, 1992; Fisher and Anastasio, 1994; Homza and Wallace, 1995, 1997; Anastasio et al., 1997; Thorbjornsen and Dunne, 1997). These studies tested and improved the early kinematic models of fault-related folding (e.g. Suppe, 1983; Suppe and Medwedeff, 1984), resulting in a diversity of current models that employ a wide variety of simplified fold kinematics (e.g. Jamison, 1987; Suppe and Medwedeff, 1990; Erslev, 1991; Epard and Groshong, 1995; Homza and Wallace, 1995; Ford et al., 1997; Hardy and Ford, 1997; Spang and McConnell, 1997; Suppe et al., 1997). Many of these models have proven highly useful in predicting fault-related fold forms from limited geometrical data. From a practical standpoint, the recognition of consistent relations between deformation patterns and fold kinematics has recently led exploration and research geologists to predict deformation patterns from kinematic histories derived from cross-section restoration principles and geometric models of fault-related folding (e.g. Apotria et al., 1996; Cacas et al., 1996; Gibbs et al., 1997; Hennings and Olson, 1997; Salvini and Storti, 1997).

Quantitative mechanical models and experimental work has firmly established that the properties of folded layers influence folding processes and products. Properties considered in many of these analyses include layer thicknesses, rheologies, competence contrasts and interface characteristics (e.g. Biot, 1961, 1965; Ramberg, 1961, 1964; Currie et al., 1962; Ramsay, 1967; Hudleston, 1973; Chapple and Spang, 1974; Johnson, 1977; Hudleston and Holst, 1984; Tanner, 1989; Hudleston and Lan, 1994). The influ-
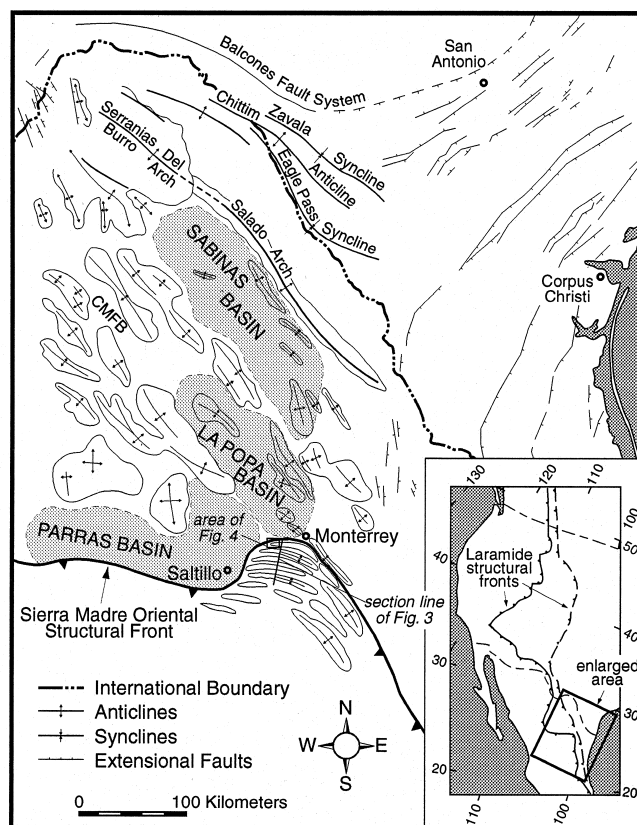

Fig. 1. Regional location map showing distribution of major tectonic features in northeastern Mexico. CMFB = Coahuila Marginal Folded Belt. Modified after Wall et al. (1961), Weidie and Martinez (1970), McBride et al. (1974), and Gray and Johnson (1995).

ences of these various properties are manifest not only in geometrical aspects such as fold wavelength, the shape of folded layers and the harmony of folded multilayers, but also in mechanical aspects such as the distribution of strain throughout a folded layer or multilayer, the dominance of brittle or ductile deformation, and the micro- and mesoscale deformation mechanisms through which folding is accomplished.

Despite such strong theoretical and experimental evidence for a significant role of layering in folding and fold-related deformation, most models do not rigorously account for the influence of stratigraphy on any geometrical or mechanical aspect of fault-related folds. This paper documents the stratigraphic variability of deformation in a map-scale detachment fold and describes a general methodology by which to account for stratigraphic influences on fold-related deformation patterns. Ultimately, our purpose is to emphasize that even within a single structure, and at scales that are significant for reservoir characterization and hydrocarbon production, deformation mechanics and kinematics may be dramatically different in rocks with differing stratigraphic, sedimentologic or compositional characteristics. Because of this, deformation patterns
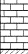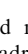
Age		Unit	Lithology, Thickness Competence		
Cretaceous	Upper	Difunta Gp.		4000 m	weak
Cretaceous	Upper	Parras Shale		1500 m	weak
Cretaceous	Upper	San Felipe		1500 m	weak
Cretaceous	Upper	Auga Nueva		150 m	weak
Cretaceous	Lower	Cuesta del Cura		60 m	weak
Cretaceous	Lower	Aurora		200 m	strong
Cretaceous	Lower	La Pena		25 m	weak
Cretaceous	Lower	Cupido		830 m	strong
Cretaceous	Lower	Taraises		270 m	weak
Jurassic	Upper	La Casita		800 m	weak
Jurassic	Upper	Olvido		50 m	weak
Jurassic	Upper	Zuloaga		200 m	strong
Jurassic	Upper	Minas Viejas		1000 m	weak

Fig. 2. Regional stratigraphy and mechanical stratigraphy of the Monterrey salient of the Sierra Madre Oriental. Unit thicknesses are regional averages taken from Goldhammer et al. (1991).

may be dramatically different in geometrically identical structures with similar kinematic histories, or in adjacent stratigraphic intervals in the same structure, due largely to the effects of differing stratigraphy.

2. Regional geology

The regional setting for our study is a salient in the Sierra Madre Oriental (SMO) between Saltillo and Monterrey, Mexico, a small segment of the Laramide deformation belt that extends discontinuously throughout almost the entire North American continent (Fig. 1). In contrast to areas west of Saltillo and south of Monterrey, where the SMO is dominated by classic fold–thrust structures (e.g. Quintero-Legorreta and Aranda-Garcia, 1985; Suter, 1987), deformation in the Monterrey salient is dominated by a series of folds with few mapped faults (e.g. de Cserna, 1956; Wall et al., 1961; Weidie and Murray, 1967; Padilla y Sanchez, 1982). These folds involve a 3000 m thick sequence of Upper Jurassic through Cretaceous carbonates and siliciclastics that are detached above an evaporite sequence whose initial thickness is estimated at 1000 m (Fig. 2; Goldhammer et al., 1991). Above this detachment, the remainder of the regional stratigraphy can

be loosely divided into a series of six alternating competent and incompetent mechanical units (Fig. 2).

The Monterrey salient is bounded to the west by the Parras Basin, to the north by the La Popa Basin and to the northeast and east by the Coahuila Marginal Folded Belt (Fig. 1; Wall et al., 1961; McBride et al., 1974). The Parras and La Popa Basins contain up to 5400 m of Upper Cretaceous to Paleocene sedimentary rocks deposited in a series of prograding and retrograding deltaic complexes derived from western and southwestern sources (McBride et al., 1974). In these basins, the rocks are complexly thrust faulted and folded into north- and south-verging structures that are commonly interpreted to root in a Parras Shale detachment (McBride et al., 1974; Dillman, 1985; Taylor, 1993).

In the Coahuila Marginal Folded Belt, Cretaceous carbonates are exposed in narrow, upright, frequently evaporite- or salt-cored anticlines that are widely separated by broad, flat-bottomed synclines floored by Upper Cretaceous clastics (e.g. Wall et al., 1961; Weidie and Murray, 1967). Similar, somewhat more axisymmetric, diapiric gypsum domes also occur within the La Popa Basin and root to the regional Minas Viejas evaporite detachment (Weidie and Martinez, 1970; Laudon, 1984; Taylor, 1993). The presence of carbonate banks within Difunta Group rocks along the flanks of many of these diapiric structures suggests these folds were bathymetrically expressed and perhaps actively growing during deposition of Difunta Group rocks (Stabler and Marquez, 1977). Consequently, although Laramide deformation in the SMO did not commence until the Eocene (Gray and Johnson, 1995), the regional evaporite detachment may have been mobile as early as the Upper Cretaceous. Because Difunta Group rocks are not preserved in synclines of the SMO, it is unknown whether SMO folds were growing diapirically prior to Laramide deformation, whether these structures developed beneath a submarine or subareal environment, or even if Difunta Group strata were ever deposited over the SMO. These questions are critical for constraining the temperature and pressure conditions of SMO folding and are beyond the scope of this paper.

Previous work has shown that folds in the SMO are upright, roughly symmetric, box-style folds with limbs that are vertical or slightly overturned (de Cserna, 1956; Padilla y Sanchez, 1982). Individual fold hinges are arcuate in plan view, and many can be traced 40–60 km. Fold wavelengths range from 4 to 7 km, and amplitudes average 2–3 km (Padilla y Sanchez, 1982). Details of the regional structural geometry are incomplete because of the lack of control on essential subsurface variables such as the depth to detachment, and a paucity of precise geologic maps. Most mapping in the SMO has been done by remote sensing (e.g. Mitre-
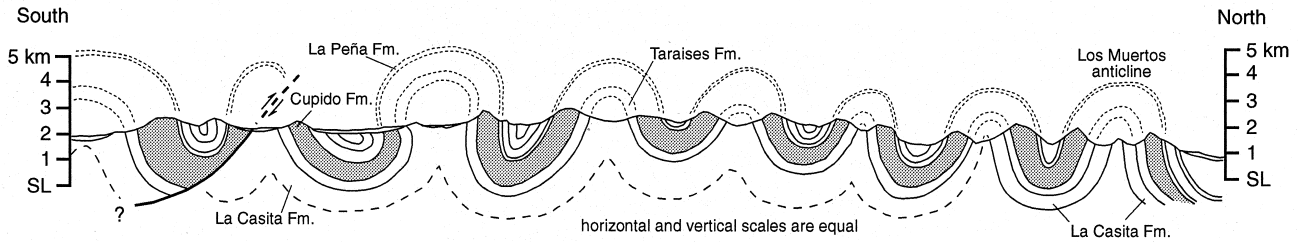
Fig. 3. Regional cross-section through the western portion of the Monterrey salient. See Fig. 1 for approximate location of section line. This is a simplified version of section E–E′ of Padilla y Sanchez (1982). Note the lack of control on deeper structural geometries.
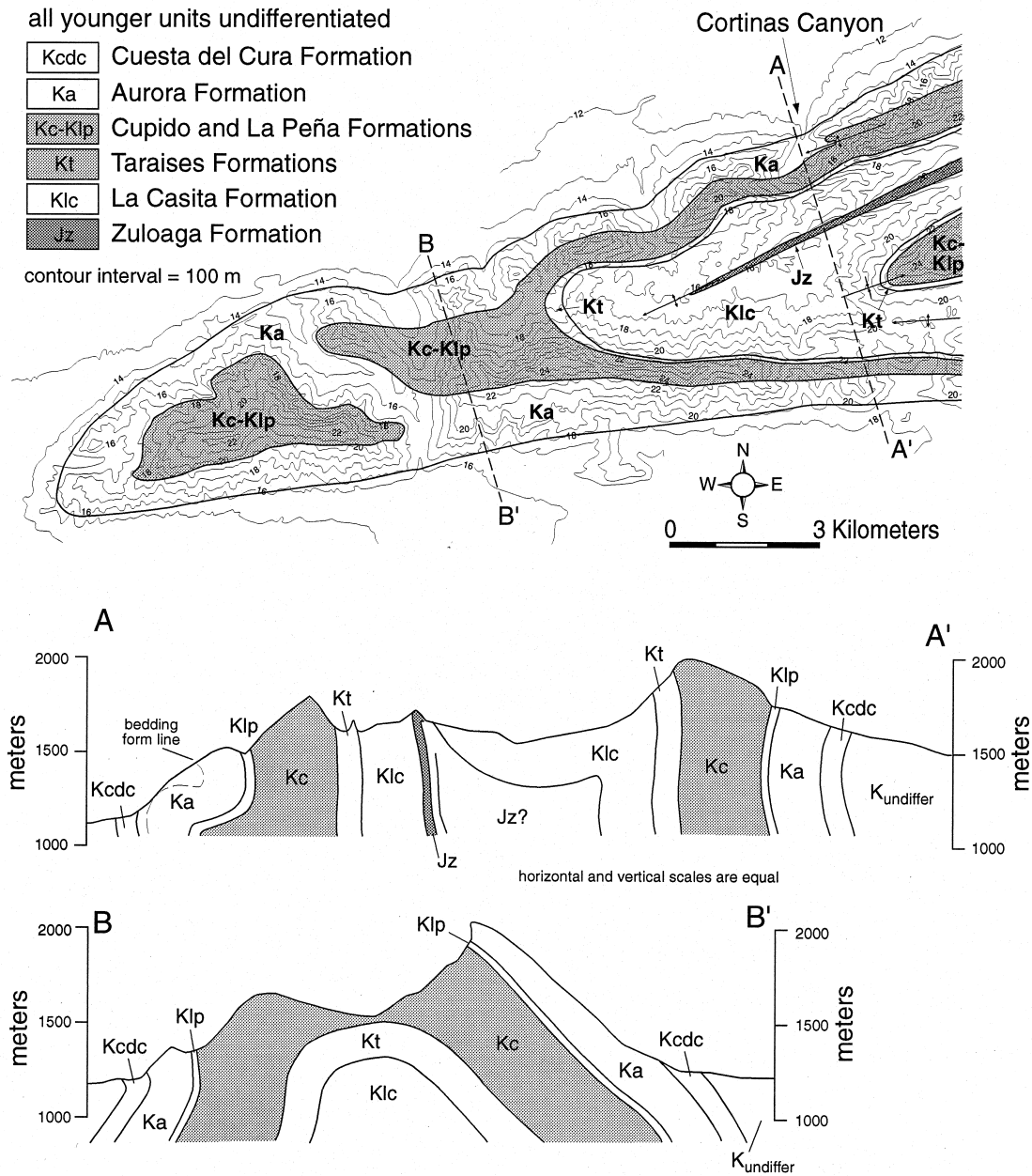
Fig. 4. Simplified geological map and Humphrey's cross-sections through the Nuncios fold complex (Humphrey, 1949). Note that map and cross-section scales are not equal. See Fig. 1 for location of map in the regional setting.

Salazar, 1981; Johnson et al., 1991), or by compilation of regional reconnaissance data into 1:200 000 or 1:250 000 scale maps (e.g. Padilla y Sanchez, 1982); few geologic maps at scales larger than this exist. Consequently, most cross-sections through the area are largely schematic and do not rigorously reconstruct subsurface geometries (e.g. Fig. 3).

3. Local geology

We conducted our study near the western termination of the frontal fold of the Sierra Madre Oriental because of the quality of exposure, ease of access, and wealth of both stratigraphic and structural work carried out in the area. At its western termination, this frontal anticline is an upright, cylindrical fold that plunges approximately 15° toward the WSW (Fig. 4). Along strike towards the east, the crest of the fold is broad and flat, and eventually sags, creating a synclinal depression that increases in amplitude and continues along strike for several tens of kilometers. This syncline separates what is a single fold in the west (Section B–B′ in Fig. 4) into a pair of anticlines with an intervening syncline towards the east (Section A–A′ in Fig. 4). This transition in structural geometry occurs gradually over a distance of 10–15 km.

Without the benefit of topographic base maps, Humphrey (1949) mapped the western end of this fold complex at a scale of 1:50 000, and named the northernmost anticline the Los Muertos anticline. Because Humphrey's place name of Muertos does not figure prominently on modern topographic maps, however, we previously referred to the entire three-fold structure as the Nuncios fold complex (Fischer et al., 1996), naming the structure after the currently recognized mountain, Sierra San Jose De Los Nuncios, where the fold is exposed at the western termination. We herein retain that naming scheme, using the name Nuncios to refer to the entire three-fold complex, and using the name Muertos to refer only to the frontal anticline in areas where there is a distinct and prominent intervening syncline (e.g. immediately south of Monterrey).

4. Approach and rationale

We collected structural and stratigraphic data along a transect across the entire Nuncios fold complex (Fig. 4). In this paper we present data from rocks exposed in Cortinas Canyon, a deeply incised cross-strike drainageway in the northernmost limb of the Nuncios fold (Fig. 4). Cortinas Canyon provides unrestricted access to subvertically oriented rocks from the Zuloaga Limestone through the Aurora Formation (e.g. Humphrey, 1954; Goldhammer et al., 1991; Gray and Johnson, 1995).

By restricting our work to one structural position in the fold, we hope to factor out structural and environmental influences on the observed deformation patterns. The forelimb rocks exposed in Cortinas Canyon probably underwent similar kinematic histories, and burial depths are unlikely to have varied by more than the thickness of the section (i.e. < 2 km). Initial differences in burial depth were continually reduced during uplift and folding, as the rocks examined are currently separated by less than 300 m of elevation. Mechanical and geochemical fluid–rock interactions may have played a significant role in controlling the observed deformation patterns, and our data suggest the presence of notable fluid boundaries or conduits at certain parts of the stratigraphic section. Aside from the recognition of these boundaries and their correlation with certain stratigraphic factors, however, detailed analysis of the role of fluids in the deformation is beyond the scope of this paper.

After factoring out structural and environmental influences, we interpret that observed deformation patterns are largely controlled by stratigraphic factors. If stratigraphy played no role in controlling deformation, then under similar environmental conditions, all rocks with similar structural histories should exhibit the same style, intensity and distribution of deformation. This is not true in the forelimb of the Nuncios fold complex, where deformation patterns vary strongly between rock types. Establishing consistent correlations between deformation and stratigraphy will facilitate predictions of deformation patterns from stratigraphic data.

We present our correlations between stratigraphy and deformation in the form of a mechanical stratigraphy (e.g. Corbett et al., 1987; Gross, 1995; Gross et al., 1997c), wherein each mechanical unit is defined as a specific stratigraphic interval that consistently displays a characteristic set of deformation features; each mechanical unit exhibits a characteristic deformation response that is dictated by stratigraphic factors.

5. Mechanical stratigraphy in Cortinas Canyon

Definition of mechanical units depends on the scale of observation. At the regional scale, we recognize six units above the Minas Viejas evaporite detachment (Fig. 2). These units are distinguished by their bulk response to deformation using the generally accepted idea that pelitic rocks are more easily deformed than carbonates. The lower five mechanical units are exposed in Cortinas Canyon, and we now present detailed descriptions of the internal mechanical stratigraphy of the formations comprising each of these units, in most cases subdividing them into thinner mechanical units. The thickness of these subdivisions
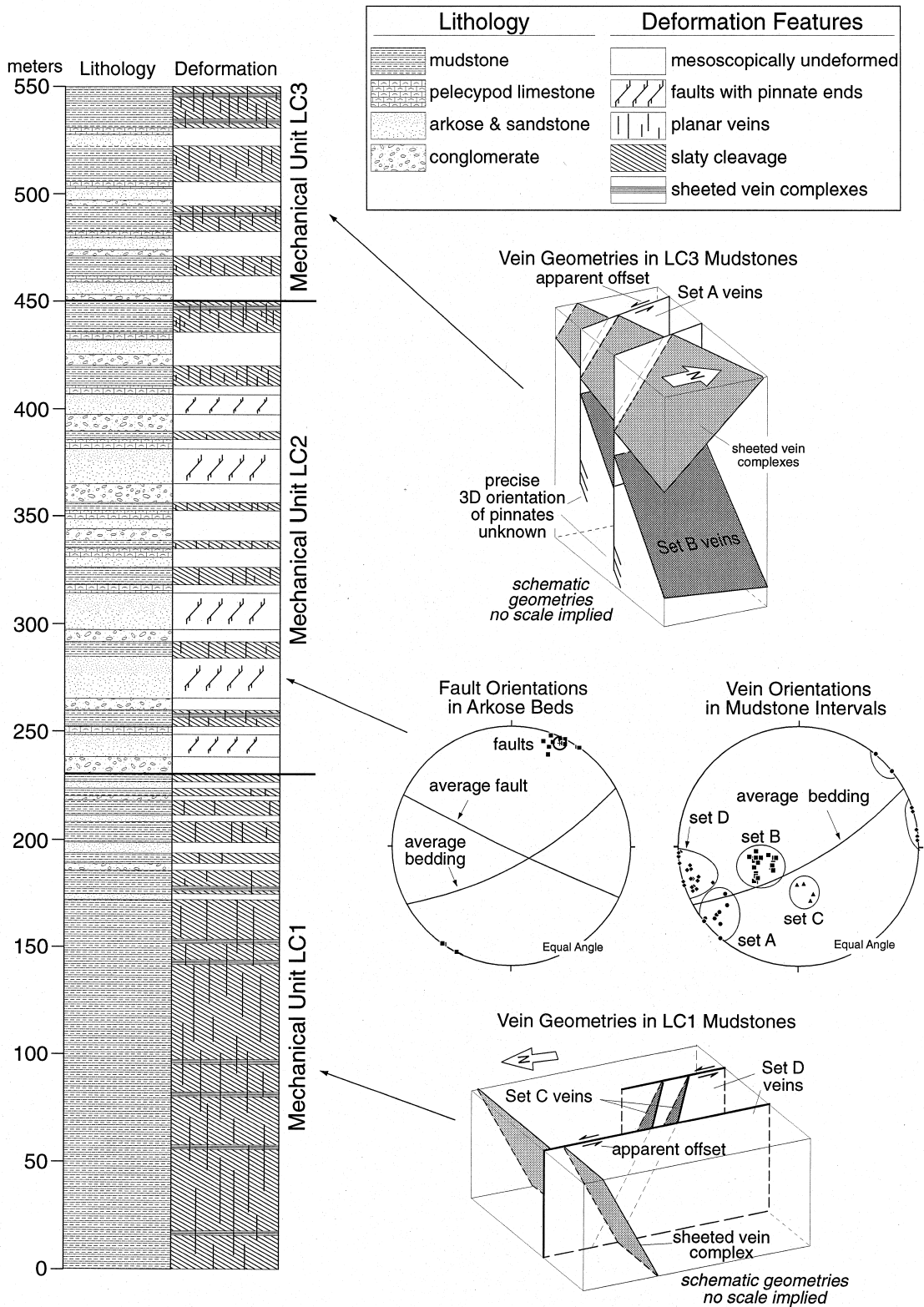
Fig. 5. Generalized lithofacies and mechanical stratigraphy of the La Casita Formation. Layer thicknesses in the lithology column are schematic, meant only to show relative abundances and depositional sequences of various lithologies. The column representing deformation is likewise schematic; thicknesses, exact vertical position and cross-cutting relations are not intended to be representative of outcrop characteristics. Relative abundances and distributions of various fabrics and deformation features are correctly represented. Box diagrams depict general geometries and cross-cutting relations between various vein sets. Stereoplots depict orientations of veins developed in mudstone intervals and faults developed in arkose layers. The average pole to these faults is marked by a plus sign in the center of the corresponding 95% confidence cone. Note that perspective vantage point differs in each box diagram.

varies from less than a meter to over a hundred meters. For each formation we first provide a general stratigraphic description, followed by a more detailed discussion of the structural and stratigraphic correlations seen in that unit.

5.1. Zuloaga Formation

The Zuloaga Formation is exposed at the head of Cortinas Canyon where it occupies the hinge zone of the Muertos anticline (Fig. 4). Because this unit occupies the hinge of the fold, the observed deformation features may in part be due to a different kinematic history from rocks further north in Cortinas Canyon. We nevertheless provide a description of the Zuloaga Formation, because throughout the Monterrey Salient, this unit is rarely found in outcrops that are not in fold hinge zones. Thus, our observations characterize the deformation response of the formation in its typical structural position. Detailed descriptions of the stratigraphy and petrography of the Zuloaga Formation are given by Ovianki (1974), Meyer and Ward (1984), Finneran (1986) and Johnson (1991).

The Zuloaga Formation at this location is structurally and stratigraphically complex. Discontinuous, irregular breccia bodies over several hundred cubic meters in volume pervade the outcrop and bedding is not readily discernible. Outside of the breccia bodies, the unit is comprised of two dominant microcrystalline lithofacies: dark gray to black, dolomitic limestone and medium gray limestone. Boundaries between these units are commonly irregular and distorted and individual facies often abruptly pinch out or truncate along strike in less than ten meters. Limestone units typically contain prominent subvertical stylolites with amplitudes of 10–15 cm and spacings of 30–60 cm. These stylolites are absent in darker, dolomitic units, that instead contain subvertical, sparry calcite veins that do not extend into lighter limestone units.

The breccias are comprised of angular to subrounded clasts with diameters ranging from 0.01 to 2 m, and a matrix of dark gray, microcrystalline limestone and blocky calcite vein material. Clasts of both carbonate lithofacies are present in the breccias, as well as tan to orange–brown, weakly calcareous mudstone similar to that found in units directly overlying the Zuloaga Formation and exposed less than 50 m to the south. Vein material occurs within subplanar cracks across larger clasts, and within the breccia matrix as irregular fill, some of which contains euhedral crystals that grew into open voids. Clast margins are not significantly altered or dissolved, and there is no penetrative internal deformation of the clasts or matrix.

5.2. La Casita Formation

In Cortinas Canyon the La Casita Formation can be subdivided into two dominant lithofacies and three mechanical units (Fig. 5). The lower facies consists of ∼230 m of monotonous, carbonaceous, thinly bedded, black, dark gray and occasional brown shale. Overlying this unit is ∼320 m of interbedded immature sandstone, lithic arkose, conglomerate, mudstone and limestone with abundant pelecypod shell fragments. In the upper ∼100 m of the formation, these lithologies are arranged in coarsening-upward cycles with average thicknesses of 2–3 m. Individual bed thicknesses in the upper facies vary from 0.2 to 1.5 m, with coarser beds generally becoming thinner and less abundant upwards in the section. Measured sections, petrographic and stratigraphic descriptions of the La Casita Formation are presented by Humphrey (1949, 1954), Fortunato and Ward (1982) and Smith (1987).

Deformation patterns in the La Casita Formation are strongly linked to the relative abundances and thicknesses of mudstones and immature sandstones or arkoses. Since these characteristics change gradually throughout the section, the boundaries between the three mechanical units are gradational. The lower mechanical unit (LC1) is dominantly mudstone, and contains a penetrative, continuous, slaty cleavage and two systematic sets of planar veins (Fig. 5). Because primary compositional layering is weakly developed in the mudstones, making it difficult to distinguish between this cleavage and bedding, we use the term S_0/S_1 to refer to the dominant, earliest foliation in LC1, and in all parts of the section where this distinction is similarly tenuous (e.g. the Taraises Formation).

Sheeted vein complexes (SVC) subparallel to S_0/S_1 and up to 4 cm thick are the oldest veins in LC1 because they are commonly cut and offset by subvertical to steeply east-dipping, planar, cross-fold veins (Set D in Fig. 5). The SVCs have undulose margins, and are often internally layered on a millimeter to centimeter scale, with black to dark gray insoluble horizons interleaved with quartz and sparry calcite layers. Textures in the SVCs are similar to those described by Tanner (1989, 1992), where discontinuous mineral layers are separated by insoluble selvages and often appear imbricated like horses in a duplex. The margins of the SVCs frequently expose calcite fibers oriented 20–25° from the down-dip direction of the S_0/S_1 foliation.

The cross-fold veins are planar and continuous, with many extending through 2–5 m of section. These veins are comprised of sparry calcite with minor quartz. Their typical apertures are 2–5 mm, and their perpendicular spacings range from 5 to 150 cm, but average roughly 40 cm. More prominent Set D veins with apertures greater than 1 cm always offset SVCs, and show
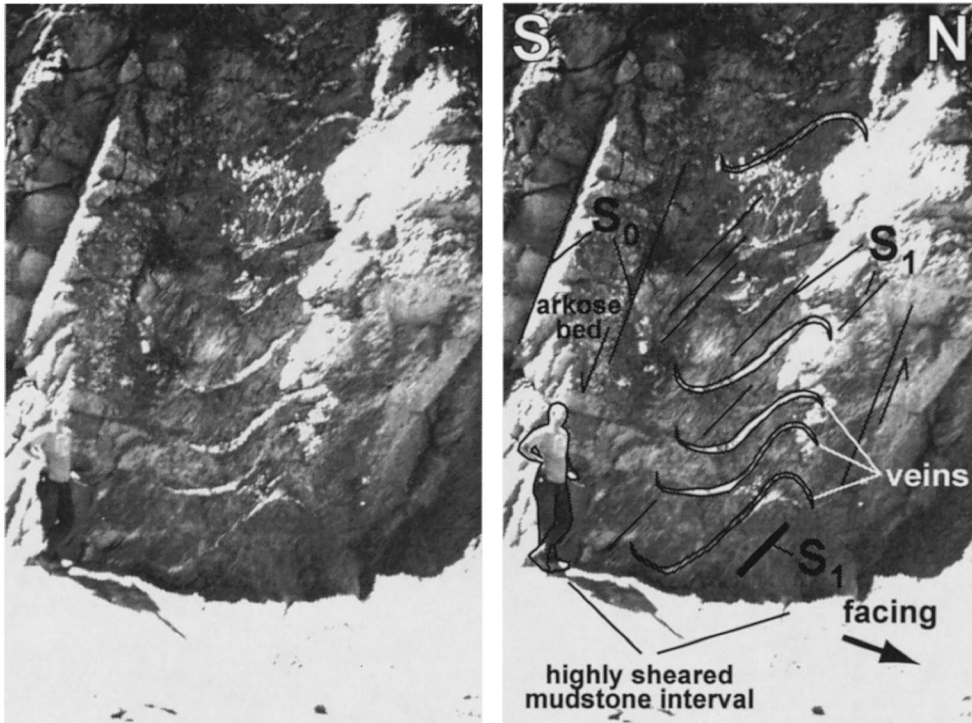
Fig. 6. Large-scale shear zone and sigmoidal en échelon vein array in mechanical unit LC2. View to west, with veins and shear zone foliation indicating north-side-up sense of motion.

a consistent sinistral sense of motion (Fig. 5). This sense of motion is also suggested for thinner veins because these commonly terminate in pinnate tails (Set C in Fig. 5) that link to neighboring parallel veins to form rhombochasms. The offsets and orientations of veins in this unit suggest the veins likely accommodated both differential cross-fold shortening, and minor hinge-parallel extension. The timing of the veins is ambiguous, but faint traces of cleavage seen in some Set D veins suggest that these veins and the SVCs in LC1 formed before or synchronously with cleavage formation.

Deformation in the middle mechanical unit (LC2) is markedly different from that in LC1 (Fig. 5). Sheeted vein complexes are rare, and Set D veins, though present, are poorly developed, more widely spaced, and confined to mudstone intervals typically less than 2 m thick. Occasionally, when bounded by sandstone beds thicker than 30–40 cm, mudstone intervals are highly sheared, with a prominent foliation and massive sigmoidal veins, both indicating a north-side up sense of motion (Fig. 6). Confined within beds of coarser material is a prominent set of mineralized faults that is not present elsewhere in the La Casita Formation. These faults are best developed in layers greater than 30 cm thick, are mineralized with sparry calcite, spaced from 30 to 150 cm, intersect bedding at an oblique angle, have apertures of 2–7 cm, and consistently display a west-side to the north sense of slip as deter-

mined by pinnate veins that commonly occur at both ends of the faults (Fig. 7). This sense of slip suggests these faults kinematically accommodate hinge-parallel extension in coarser beds of the La Casita Formation, and although the timing of this extension relative to regional folding is uncertain, physical modeling of three-dimensional folding suggests hinge-parallel extension is characteristic of the last stages of fold development (Dubey, 1980).

In the uppermost mechanical unit (LC3), where mudstone intervals are thicker and coarse beds are less abundant and thinner, deformation is dominated by a prominent S_0/S_1 fabric, sheeted vein complexes similar to those in LC1, and two sets of planar, cross-fold calcite veins (Sets A and B in Fig. 5). Set B veins in LC3 not only exhibit spacings, apertures and continuities similar to Set D veins in LC1, but also offset SVCs with a west-side-to-the-south sense of motion, resulting in minor hinge-parallel extension. Set A veins in LC3 commonly display apertures less than 5 mm and trace lengths parallel to S_0/S_1 of 2–3 m. Set B veins offset by Set A veins, as well as pinnate tails on most Set A veins, indicate an east-side-up sense of motion. Similar to Set D veins in LC1, these features most likely formed to accommodate differential cross-fold shortening, and minor hinge-parallel contraction.

In general, two different histories are suggested for planar veins in the La Casita Formation. Orientations with respect to S_0/S_1, pinnate tails, and curved antitax-
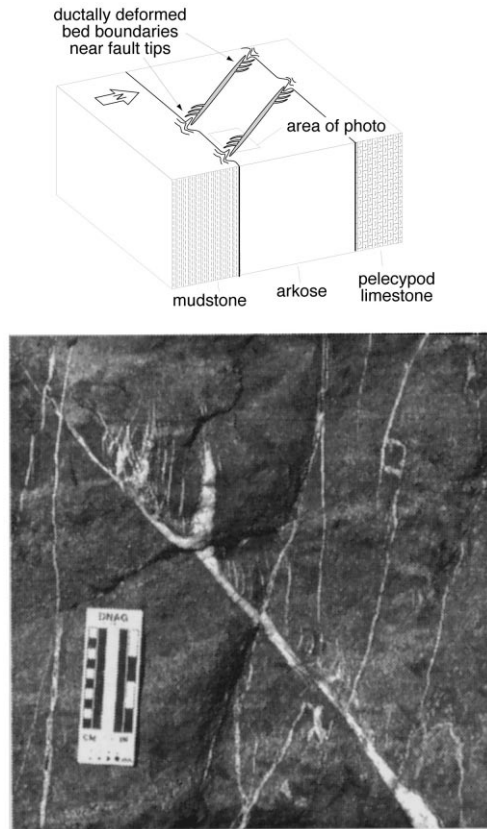
Fig. 7. Geometry of mineralized faults developed in arkosic units of LC2.

ial calcite fibers in many Set B veins suggest that these features most probably formed as shear fractures with a long history of slip, and are not simply reactivated joints. This history contrasts with Set D and C veins, whose orientation, continuity, planarity, lack of internal fabric, and pinnate tails suggest that they probably formed as cross-strike joints that were subsequently reactivated in shear.

5.3. Taraises Formation

The Taraises Formation consists of two lithofacies, each of which comprise a mechanical unit (Fig. 8). The lower lithofacies consists of ~25 m of massive, dark gray limestone with abundant pelecypod, bryozoan and coral fragments and is known as the San Juan Lentil. Although it is prominent in Cortinas Canyon and can be traced along strike for over 15 km, this carbonate buildup formed in a relatively unique depositional environment and is uncommon throughout most of the Monterrey salient. The upper mechanical unit (T2) is ~150 m of thin-bedded, black, gray and dark brown, calcareous mudstone and shale similar to mudstones in the upper part of the La Casita Formation.

More detailed descriptions of the Taraises Formation are provided by Piaggio (1961), Barrier (1977) and Blauser (1979).

Mechanical unit (T1) is the San Juan Lentil, and is deformed by a weak, spaced, wavy to anastamosing pressure solution cleavage in muddier, fossiliferous packstone and wackestone horizons. Intervals with abundant large pelecypod fragments and less matrix are typically not cleaved. Opposing pairs of calcite-mineralized, cross-fold faults extending through 3–5 m of section are also present within this unit. The faults are slickensided, and often display multiple sets of lineations, some intersecting at angles greater than 30°.

Deformation in the mechanical unit T2 is characterized by two cleavages and two sets of calcite veins. Cross-fold veins in T2 are similar to Sets A and D in LC1 in terms of composition, aperture, planarity and orientation, but typically extend through less than 2 m of stratigraphic section. Often these veins appear in groups intersecting at small angles and spaced from 10 to 40 cm. Sparry calcite veins subparallel to the dominant foliation are prominent, showing perpendicular spacings of 3–6 m, extending for 5–10 m along strike, and displaying apertures from 2 to 4 cm. These veins are similar in orientation to the sheeted vein complexes in LC1, but commonly do not display the layered internal textures seen in the LC1 SVCs.

Both the cross-fold and the foliation-parallel veins are deformed by cleavage. The cross-fold veins are cut and dissolved along a continuous, smooth, penetrative slaty cleavage like that seen in mudstones of the La Casita Formation. Because this fabric is similarly difficult to distinguish from bedding, we also refer to it as an S_0/S_1 fabric, and hereafter refer to the veins aligned with it as foliation-parallel veins. Locally, and especially in lighter and apparently more clay-rich layers, the S_0/S_1 fabric is deformed by a second (S_2), steeply north-dipping, 2–30 mm spaced, asymmetric crenulation cleavage (Fig. 8). Occasionally this crenulation occurs as isolated, 10–50 cm wavelength and 5–15 cm amplitude, asymmetric, kink folds in the S_0/S_1 fabric.

5.4. Cupido Formation

In Cortinas Canyon, the Cupido Formation is 530–640 m thick, and comprised of four major lithofacies, each of which contains a variety of subfacies ranging in thickness from less than a meter to several tens of meters (Fig. 9). The lower 40–50 m of the section is a massive to thick-bedded, dark gray, locally fossiliferous, reefal unit. Overlying this unit is 310–360 m of light gray to tan, medium- to thick-bedded, and interbedded, intraclastic wackestone, bioturbated calcareous wackestone, packstone and dark gray dolomitic wackestone. The third lithofacies is 60–80 m of med-
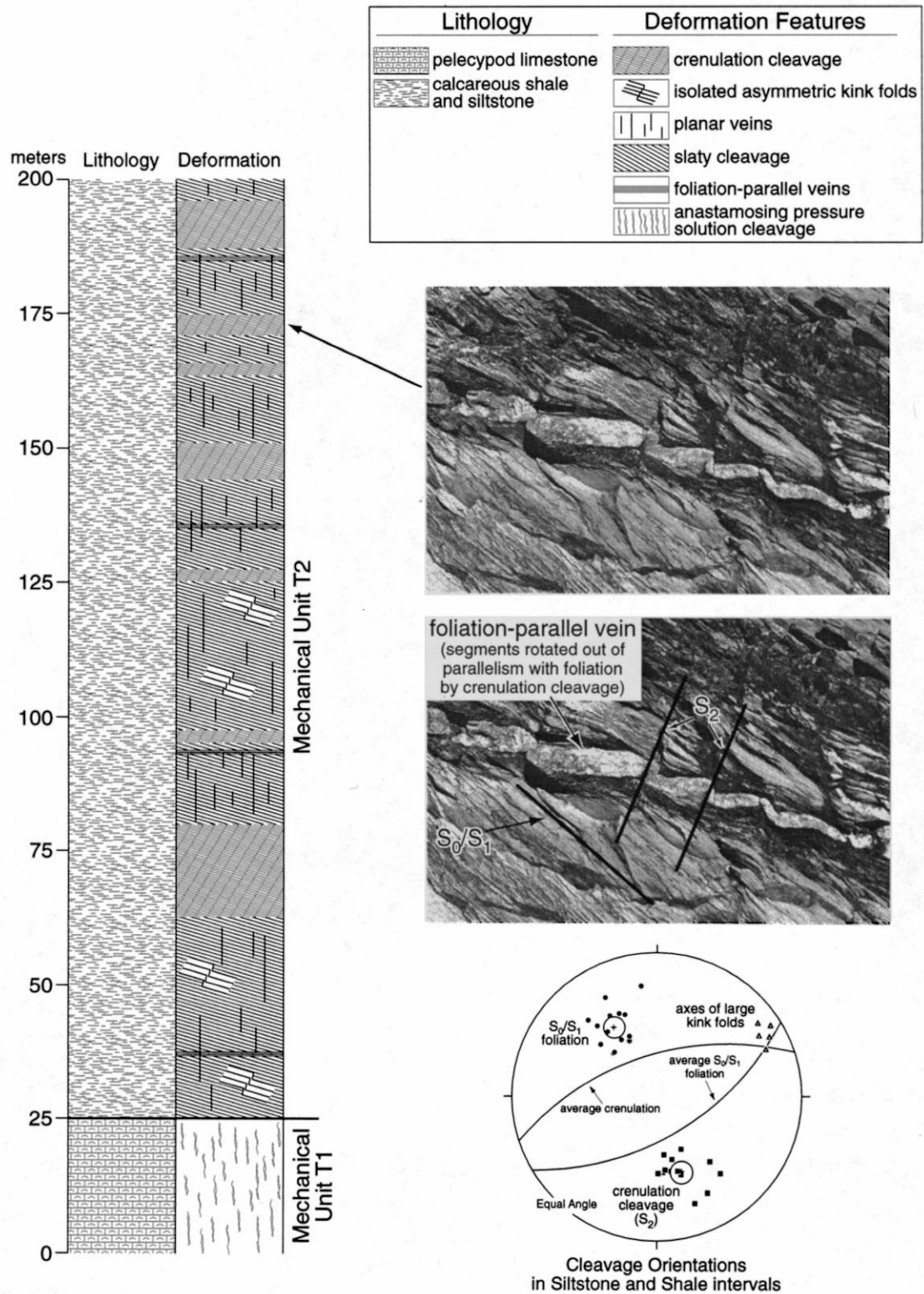
Fig. 8. Generalized lithofacies and mechanical stratigraphy of the Taraises Formation. The column representing deformation is schematic; thicknesses, exact vertical position and cross-cutting relations are not intended to be representative of outcrop characteristics. Relative abundances and distributions of various fabrics and deformation features are correctly represented. Uninterpreted and interpreted photos of crenulation fabric in unit T2 are illustrative of typical fabric geometries and relations in that unit. View in the photo is along strike toward the northeast. Stereoplot depicts the orientations of S_0/S_1 foliation, S_2 crenulation, and axes of asymmetric kink folds developed in mechanical unit T2 and described in the text. Average poles to the foliation and crenulation are shown as a plus sign in the center of their corresponding 95% confidence cone.
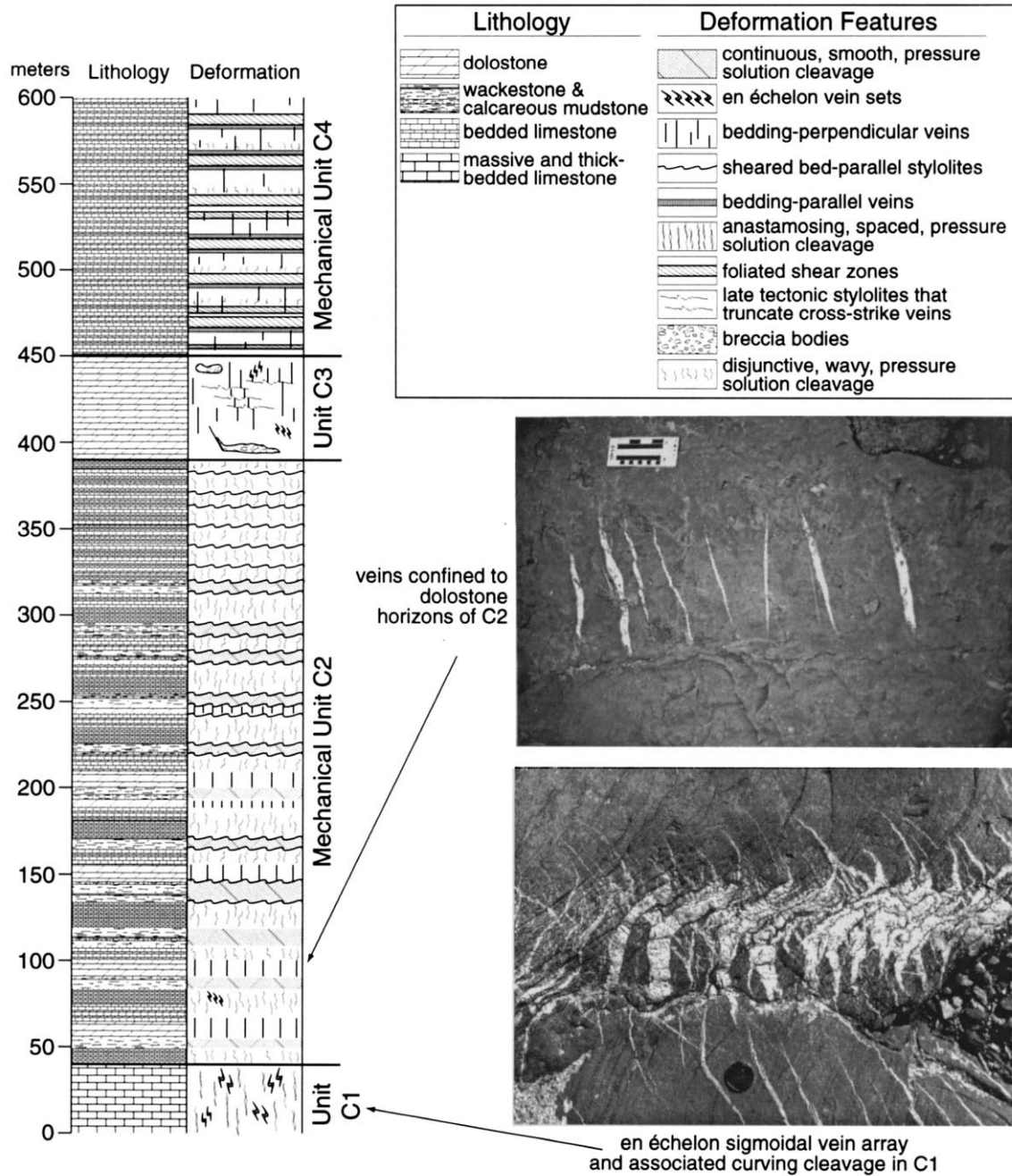
Fig. 9. Generalized lithofacies and mechanical stratigraphy of the Cupido Formation. Layer thicknesses in the lithology column are schematic, meant only to show relative abundances of various lithofacies. The column representing deformation is likewise schematic; thicknesses, exact vertical position and cross-cutting relations are not intended to be representative of outcrop relations. West is to left in upper photo. North to right in lower photo.

ium-bedded, dark gray to black, dolomitic wackestone. The uppermost 120–150 m of the formation is informally known as the Cupidito (Wilson and Pialli, 1977; Wilson, 1981), and is comprised of well-bedded, medium-bedded, light to dark gray packstones and wackestones. Although each major lithofacies defines a mechanical unit, similar subfacies in different mechanical units also commonly display consistent defor-

mation patterns. More complete discussions of Cupido Formation stratigraphy, facies, depositional environments, average thicknesses, and petrography are provided in Conklin and Moore (1977), Wilson and Pialli (1977), Wilson (1981), Selvius (1982), Wilson and Selvius (1984) and Wilson and Ward (1993).

Dominant structures in the lowest mechanical unit (C1) include a wavy, 3–7 mm spaced, pressure solution

Fig. 10. Geometries and orientations of en échelon vein arrays and pinnate veins observed in the unit C1 of the Cupido Formation. Arrays are divided into five groups 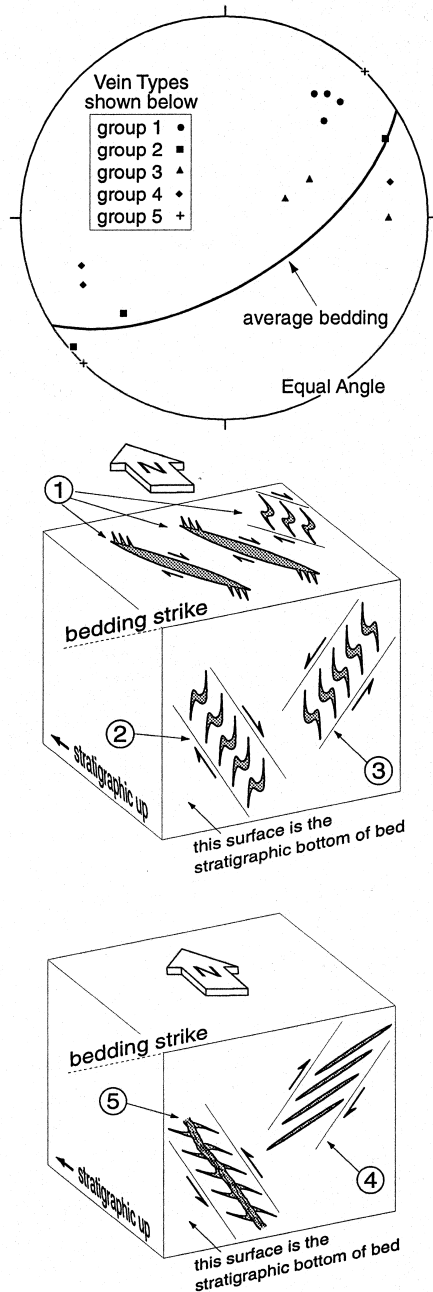based on their kinematic effect on bedding, orientation and style. The stereoplot illustrates a representative sampling of the orientations of each of the five array types. Block diagrams illustrate the style and geometry of each vein or array type in its currently observed field geometry, where the circled number pointer corresponds to the group type in the stereonet.

Fig. 11. Sheared bed-parallel stylolites and weak, southeast-dipping, disjunctive pressure solution cleavage in the upper parts of Cupido mechanical unit C2. Note that stylolite teeth lie in the plane of the cleavage, as illustrated by a few representative data in the stereoplot. Photo view is along strike toward the southwest. Ten Peso piece for scale.

cleavage, and at least five types of calcite vein arrays and pinnate cross-fold veins that can be grouped according to their orientation and kinematic effect on bedding (Fig. 10). Groups 1, 2 and 3 accommodate hinge-parallel extension, whereas groups 4 and 5 ac-

commodate hinge-parallel contraction. All of the vein arrays cross-cut one another and are locally so abundant that they account for 10–15% of the total rock volume. Though not well-constrained, the dimensions and amount of vein rotation within many of the arrays suggest that they had a long period of activity. Because cleavage is rotated and intensified within many of the vein arrays, we interpret that the arrays formed after or during the latest stages of cleavage for-

mation (see lower photo in Fig. 9). Finally, the concentration of vein arrays near the Cupido–Taraises contact suggests that this contact was important in controlling fluid migration. It may have been a migration pathway through which large volumes of fluid passed from the Taraises Formation and deeper stratigraphic levels, or a migration barrier that was repeatedly fractured and faulted with the aid of overpressured fluids beneath it. Stratigraphically upward from this boundary, the vein arrays quickly become less common and give way to a new deformation pattern in the overlying mechanical unit.

Deformation in mechanical unit C2 varies between interbedded and well-bedded facies of contrasting lithology. The thickness of individual facies in this interval ranges from 0.3 to 2 m, and the character of cleavage and bedding-parallel stylolites is markedly different in each facies. Tan to brown, mottled, bioturbated and intraclastic facies contain spaced, wavy or anastamosing cleavage, whereas adjacent light gray wackestone units contain 10–15 cm spaced, stylolitic cleavage. Boundaries between these facies are marked by prominent stylolites with amplitudes of 15–20 cm, and which curve asymptotically into the intraclastic facies.

Stratigraphically upward in mechanical unit C2, individual facies thicknesses gradually decrease, and the intraclastic facies is replaced by orange–brown wackestone and dark gray, dolomitic wackestone and dolostone. The dolomitic horizons are uncleaved, but contain a regularly spaced set of planar, cross-fold, sparry calcite veins with apertures from 5 to 25 mm. The veins are confined to dolomitic horizons, and frequently terminate against 5–10 mm amplitude, wavy, stylolitized facies boundaries. The light gray wackestone facies contains wavy or anastamosing, 2–5 mm spaced pressure-solution cleavage that maintains its orientation across the unit. In contrast, orange–brown wackestone units commonly display continuous, smooth cleavage that is steep near the centers of beds and asymptotically curves toward the bed boundaries.

The uppermost portions of unit C2 are almost exclusively well-bedded, light gray wackestones. These units display irregular, 5–10 cm amplitude, stylolitic bed boundaries and weak, 3–7 cm spaced, wavy to anastamosing pressure-solution cleavage. As shown in Fig. 11, stylolite teeth are inclined to bed boundaries and lie in the cleavage plane. As noted by Treagus (1988) and Bamford and Ford (1990), this relationship could arise by at least two mechanisms. In one case, cleavage initiates prior to significant folding as a bedding-perpendicular, layer-parallel shortening (LPS) fabric. This fabric is then passively rotated during hinge-directed shear. In the second case, cleavage forms under shear during folding, and reactivated pressure solution along the stylolites causes them to undergo volume loss flat-

tening and align with cleavage. Because we found no evidence for reactivation and flattening of the stylolites such as a consistent asymmetry in selvage thickness, we interpret that this cleavage is an early LPS fabric.

The third mechanical unit (C3) in the Cupido Formation is dark gray to black dolomitic wackestone and dolostone with several subfacies as thin as 3–4 cm. Cleavage is absent here, and boundaries between subfacies in this unit are undulose, gradational and not stylolitized. En échelon arrays of sigmoidal calcite veins similar to group 1 arrays in mechanical unit C1 are also present in C3, but in markedly less abundance (Fig. 9). Planar faults oriented like group 1 pinnate veins in C1 are likewise present in C3, but instead of ending in pinnate tails, these faults frequently sole out into brecciated and mineralized bed-parallel horizons. The orientations of both the faults and vein arrays indicate that they accommodated hinge-parallel extension. Similar kinematic effects are provided by a planar set of cross-fold veins with apertures less than 2 mm and trace lengths from 1 to 3 m. These veins commonly offset facies boundaries by 3–4 cm, often with a west-side-north sense of motion. Weathering of the cross-fold veins removes the calcite fill and leaves the surfaces of outcrops with a hachured appearance. Stylolites parallel to bedding and spaced from 30 to 40 cm are the last feature to form in this unit. Cross-fold veins offset by pressure solution along these stylolites suggest that 8–12 cm of material may have been removed along each stylolite (see unit C3 in Fig. 9).

Deformation in the uppermost mechanical unit (C4) is strongly influenced by the well-bedded character of this unit, and is notably different in the two common subfacies. Light gray algal wackestone units are usually uncleaved, except where adjacent to orange–tan mudstone units, where the wackestones exhibit a weak, anastamosing, 3–10 mm spaced, pressure-solution cleavage. Mudstones exhibit a continuous, wavy cleavage that may be subparallel to bed boundaries, or curve sigmoidally across a layer, intersecting bedding at a greater angle in the middle of beds and asymptotically curving parallel to bed boundaries. Often a single horizon might contain two or three 10–20 cm wide zones of curved cleavage, giving the appearance of a mesoscopic S–C fabric (Lister and Snoke, 1984). The perpendicular spacing between these foliated zones is determined by the distribution of the mudstone facies, and averages 3–5 m.

Bedding-parallel veins, cross-fold or slightly strike-oblique veins and joints are the other primary deformation features in unit C4. The presence of joints in this interval is noteworthy because this is the lowest stratigraphic occurrence of well-developed, systematic, unfilled fractures that we observed. Bedding-parallel calcite veins are poorly developed, but they are most common within or along the margins of mudstone hor-

izons, where they are 5–10 mm thick and have wavy, pressure solved boundaries. The cross-fold calcite veins are planar, exhibit apertures from 0.5 to 4 cm, and trace lengths of 2–5 m when measured along a bedding plane. Cross-cutting relations between fabrics and veins in C4 indicate that some cross-fold veins are the oldest, followed by the coeval development of bedding-parallel veins, foliated slip zones and cleavage. The last structures to form are uncommon, 20–30 cm aperture, cross-fold 'veins' that are filled with orange–brown, laminated, botryoidal calcite that locally encases angular fragments of wall rock. These structures cut all other features in C4, and may have formed from an extended period of dissolution (karstification?) and subsequent reprecipitation along a set of cross-fold joints.

5.5. La Peña Formation

At this location, the estimated thickness of the La Peña Formation is 25–30 m, and it is comprised of dark gray to black or brown shales and calcareous shales interbedded with minor light gray wackestone. Detailed stratigraphic characteristics of this formation are difficult to establish in Cortinas Canyon because it is poorly exposed. Full descriptions of the La Peña Formation are provided by Humphrey (1949), Bishop (1972), Tinker (1982), Cantu-Chapa (1989), Carrillo-Martinez (1989) and Clowes (1990).

Where exposed near the mouth of Cortinas Canyon, the La Peña Formation outcrops in several meter- to decameter-scale, disharmonic, roughly cylindrical, close to tight, asymmetric, similar folds. These folds plunge 30–40° toward the WSW, and are interpreted to occur near the hinge zone of a first-order parasitic fold developed in the forelimb of the Nuncios fold complex (Fig. 4). Because of limited exposure, and the possibility that this local parasitic folding has complicated the typical deformation response of the La Peña Formation in the forelimb of the Nuncios fold complex, we cannot provide a definitive description of the behavior of this unit. However, the general character of deformation, coupled with the presence of abundant shales that can clearly detach from, and deform independently of neighboring units, leads us to interpret that the La Peña Formation probably serves as a minor regional detachment horizon. In support of this interpretation, folding and faulting within this unit is seen at many outcrops throughout the Monterrey salient, for example, along Mexican Highway 57 where it passes through Cañon del Chorro near Arteaga.

5.6. Aurora Formation

In Cortinas Canyon the Aurora Formation is 150–225 m thick, and gradually changes up-section from massive dark gray reef facies into well-bedded, light gray to blue–gray wackestones in beds from 1 to 8 m thick, but averaging 1–2 m. In the middle and upper portions of the unit shaley interbeds from 3 to 5 cm thick are found between thick limestone beds. More detailed discussions of various stratigraphic aspects of the Aurora Formation are presented in Humphrey (1949), Lozej and Beales (1977), Kindred (1988) and Wilson and Ward (1993).

Because most outcrops of the Aurora Formation in Cortinas Canyon form prominent cliffs, our accessibility to this unit was restricted. The majority of outcrops we examined were near a subhorizontal structural terrace that is part of a first-order parasitic fold in the forelimb of the Nuncios fold complex (Fig. 4). In comparing outcrops of subvertical strata on either side of the terrace with subhorizontal strata within the terrace, we noted similar deformation patterns within beds, but markedly different deformation patterns along the margins of beds.

Bed boundaries in all portions of the formation are typically stylolitic. In subhorizontal sections, bed boundaries appear welded together by 2–3 mm thick, jagged, 5–7 cm amplitude stylolitic solution seams with bedding-perpendicular teeth. In subvertical sections, stylolites are locally destroyed and replaced by 5–15 cm thick, red–orange clay-rich layers containing brecciated wall rock, and discontinuous, 5–10 mm thick, undulose, bedding-parallel calcite veins with slickenlined walls. The perpendicular spacing of breccia zones can vary from 1 to 15 m, and when the zones are widely spaced, teeth of stylolitic boundaries separating beds between the zones are slightly inclined to bedding. These inclined teeth indicate a top-towards-the-hinge sense of shear similar to stylolites in mechanical unit C2 of the Cupido Formation.

Deformation within beds of both subhorizontal and subvertical sections is limited to a well-developed systematic set of cross-fold calcite veins. Cut by bed-parallel breccia zones and stylolites, the veins are early features whose bed-perpendicular height is determined by the beds containing them. The veins are subvertical, perpendicular to bedding, spaced from 30 to 250 cm, and subparallel to strike-oblique veins in the uppermost mechanical unit (C4) of the Cupido Formation.

6. General deformation sequence

The distribution and relative timing of mesostructures in Cortinas Canyon suggest the following deformation sequence during formation of the Nuncios fold complex.

1. Layer-parallel shortening, as suggested by the parallelism of cleavage and bedding-parallel stylolite
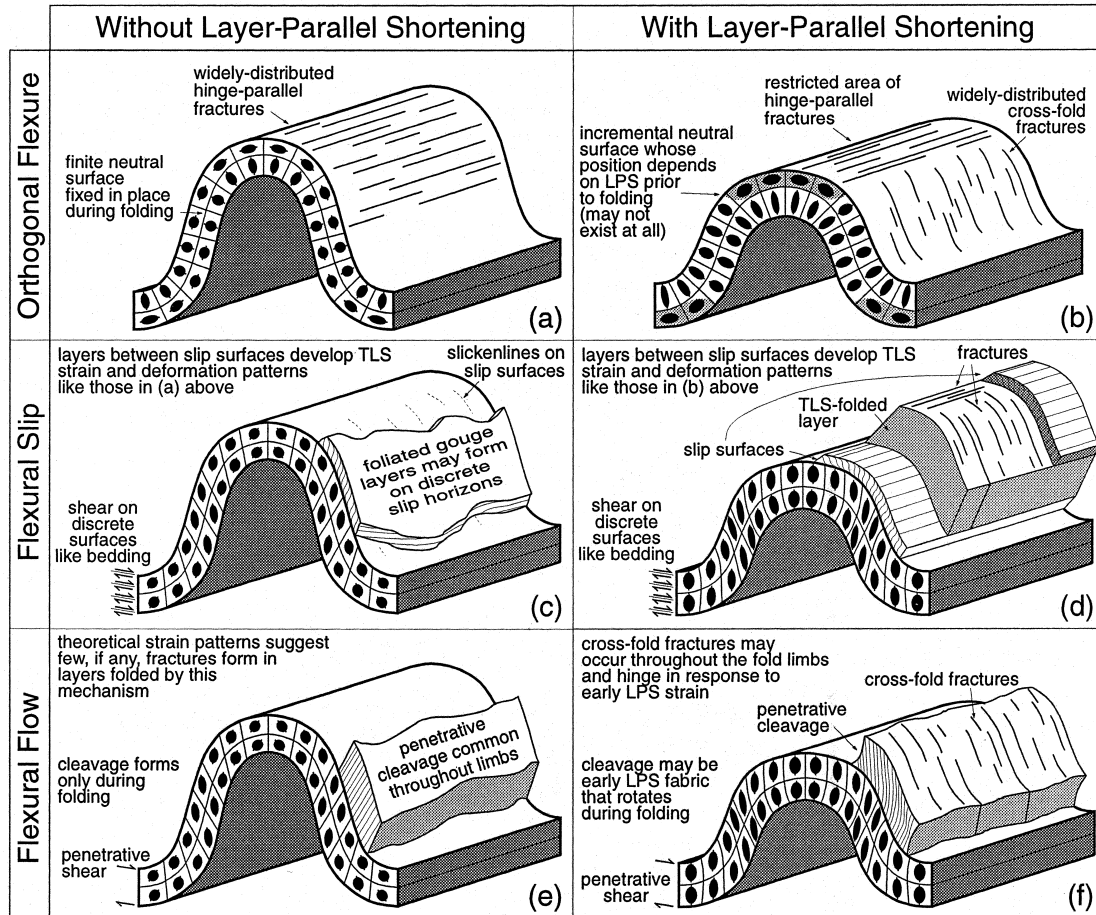
Fig. 12. Contrasting theoretical strain and deformation patterns in single-layer folds formed by flexural slip, flexural flow, and orthogonal flexure mechanisms, with or without layer-parallel shortening (LPS). All folds begin as a horizontal layer with zero strain. (a) Orthogonal flexure without LPS. (b) Orthogonal flexure with LPS. Note that in this case, the position and even existence of the neutral surface and corresponding zone of extension near the fold hinge vary with fold tightening. The distribution of hinge-parallel fractures will be determined by the amount of fold tightening and early LPS. If LPS is significant prior to folding, then cross-fold fractures may be present across the fold hinge, and will pre-date hinge-parallel fractures. (c) Flexural-slip fold without LPS. Note that the strain pattern shown here is the bulk strain in a layer containing discrete internal slip surfaces bounding layers of finite thickness. Two possible modes of deformation along slip surfaces are illustrated. (d) Flexural-slip fold with LPS. Deformation in a layer bounded by slip surfaces is depicted. (e) Flexural-flow fold without LPS. (f) Flexural-flow fold with LPS. Note that the strain pattern here is the bulk strain in a layer containing penetrative slip surfaces. Folding is preceded by the same amount of layer-parallel shortening in cases (b), (d), and (e). Deformation patterns are schematic, and not intended to accurately depict fabric densities, cross-cutting relations or precise orientations. Strain patterns adapted from Twiss and Moores (1992, pp. 316–317).

teeth in unit C2, and the presence of early cross-fold veins in many units.

2. Fold initiation and early tightening by hinge-directed shearing. This stage of deformation is represented by bedding-parallel veins, sheeted vein complexes and cleavage. Differences of 4–7° in cleavage–bedding intersection angle, though not statistically obvious from our orientation data, are visually apparent at the outcrop, and as noted by Treagus (1988), may result from strain refraction, passive rotation of an early cleavage, or some combination of the two. The coincidence in some intervals of sheared compaction stylolite teeth and cleavage

makes us favor the second and third mechanisms.

3. Late-stage fold tightening and hinge-parallel extension. After significant limb dips were attained, layer-parallel shearing stresses diminished (e.g. Behzadi and Dubey, 1980), bedding-parallel veins and sheeted vein complexes became inactive, and were cut by additional cross-fold veins and faults that extended bedding along strike. During this time, any suitably oriented, early cross-fold veins were reactivated as minor faults that also accommodated hinge-parallel extension. Bulk flattening strain in mudstone intervals is likely to have further rotated cleavage into near parallelism with bedding

and lastly resulted in the formation of a crenulation cleavage, which may also have involved a component of top-to-the-south shear (see photo in Fig. 8).

7. Discussion

Deformation patterns in fault-related folds are currently predicted from fold kinematics and curvature or kink-bank migration histories (e.g. Lisle, 1994; Gibbs et al., 1997; Hennings and Olson, 1997). These approaches provide useful first approximations of fold-related strain, but ignore the possible influence of stratigraphy on deformation patterns. In conjunction with classic theoretical studies, mounting field evidence indicates that stratigraphy plays a major role in controlling deformation, and suggests that this simplification may no longer be necessary (e.g. Corbett et al., 1987; Gross, 1995; Gross et al., 1997b,c; Hanks et al., 1997). In fault-related folds, one way to characterize stratigraphic influences on deformation patterns is to examine how different rocks accommodate the folding process. Although incremental strain or other kinematic data may establish that fold limbs rotated, the folding mechanism by which this rotation was accomplished, for example, flexural flow, flexural slip, or orthogonal flexure (e.g. Donath and Parker, 1964; Twiss and Moores, 1992, p. 240), will play a primary role in determining the associated deformation patterns. These patterns will also be related to whether folding occurred in response to bending or buckling forces (e.g. Ramberg, 1963), or in a more general sense, to the amount of layer-parallel shortening (LPS) that occurs prior to folding.

7.1. Theoretical strain distributions and folding mechanisms

If there is no LPS, folds that form by orthogonal flexure will develop tangential–longitudinal strain patterns (TLS; Ramsay and Huber, 1987b, p. 457) like those shown in Fig. 12(a). Strain magnitudes in these folds will be positively correlated with curvature, with extension on the outer, and shortening on the inner arcs of folds. Mechanical units undergoing orthogonal flexure without LPS are likely to display prominent hinge-parallel fracture sets like those seen in many basement-cored, Laramide-style uplifts (Engelder et al., 1997). Because hinge-parallel fractures may be suppressed by high confining stresses at depth (Lemiszki et al., 1994), and strain magnitudes are directly related to fold tightness, at any given burial depth, there is likely to be a minimum interlimb angle below which hinge-parallel fractures do not develop. This angle

should be smaller in thicker and more competent units.

In the presence of LPS, mechanical units that fold by orthogonal flexure will develop theoretical TLS patterns like those shown in Fig. 12(b). Strain magnitudes in these folds will also be positively correlated with curvature, but the regions over which this correlation holds may be significantly reduced in comparison to folds formed in the absence of LPS. The degree to which curvature correlates with strain will be determined by the amount of layer-parallel shortening that accrued prior to folding. The strongest and areally most extensive correlations will occur in folds that undergo little early LPS, and hinge-parallel fractures may be common in these structures. In folds with significant LPS, outer-arc extension may be nonexistent, or may be narrowly restricted to only the most highly curved portions of the fold. Consequently, hinge-parallel fractures may be rare in these folds, but cross-fold fracture sets may be common throughout the fold limbs. As with folds without LPS, increasing burial will inhibit outer-arc extension, such that tighter folding is required to initiate hinge-parallel fracturing at greater burial depths.

Folds formed by layer-parallel flexural shear (Twiss and Moores, 1992, p. 240) will develop theoretical strain patterns like those shown in Fig. 12(c–f). For multilayered sequences, it is important to discriminate flexural slip and flexural flow mechanisms (e.g. Donath and Parker, 1964). In flexural slip, shear is partitioned into discrete horizons separating layers of finite thickness that deform internally by orthogonal flexure and develop tangential–longitudinal strain patterns (Hudleston et al., 1996). Slip horizons between orthogonally-flexed layers are likely to develop veins or fine-grained gouge that will presently inhibit fluid flow across layers, but may channelize fluid flow along layers during deformation. In flexural flow, discrete slip horizons are not present, shear is continuously distributed throughout a layer, and orthogonally-flexed layers are absent. The distinction between slip and flow is significant because units deformed by slip may develop tangential–longitudinal strain patterns in intervals between slip surfaces (see Fig. 12c and d), whereas units deformed by flow should not. Consequently, layers bounded by slip surfaces in flexural slip folds may develop hinge-parallel fractures in the hinges, or cross-fold fractures in the limbs, depending on the amount of LPS prior to folding (see Fig. 12a–d). In contrast, flexural flow folds formed by buckling may have cross-fold fractures that formed in response to early LPS in the hinges and limbs of all layers (Fig. 12f), whereas layers deformed by flexural flow without LPS should theoretically have few fractures anywhere (Fig. 12e).

Because these simple models were derived for single-

layer folds, it is important to recognize that a multi-layered sequence of rocks with varying properties is unlikely to fold by a single mechanism. Folding mechanisms in multilayers should be partitioned into different stratigraphic intervals according to the properties of those intervals. Our observations document prominent contrasts in deformation between different mechanical units, and support this idea. Moreover, our data suggest that different folding mechanisms were sequentially operative in the various units. This primarily occurs in the late stages of folding because pure orthogonal flexure and flexural shear folding mechanisms operate only up to shallow to moderate limb dips (Behzadi and Dubey, 1980). Fold tightening beyond these dips may be accomplished by homogeneous flattening, or by mass transfer of material by flow or faulting out of the rapidly collapsing fold core. This deformation will most likely be accompanied by additional slip on the basal detachment, and may lead to hinge thickening and limb thinning (Williams, 1966; Ramsay and Huber, 1987b, p. 422; Bhattacharya, 1992; Lickorish and Butler, 1996).

7.2. Folding mechanisms in mechanical units of the Nuncios fold forelimb

We now interpret folding mechanisms for each mechanical unit exposed in Cortinas Canyon based on the style, distribution and intensity of deformation fabrics, as well as the relative timing of fabric development. We apply the term flexural flow in situations where shearing is obvious, but discrete slip surfaces are not visible at the outcrop scale.

Pervasive brecciation in the Zuloaga Formation indicates that folding in this mechanical unit was accomplished by a mechanism involving large strains in the fold hinge, most likely orthogonal flexure. The lack of penetrative cleavage and the presence of only widely spaced stylolites suggests that there was little LPS prior to folding of this unit.

Flexural flow, flexural slip and orthogonal flexure mechanisms were all active in the La Casita Formation, with partitioning of these mechanisms largely controlled by the distribution of mudstone and coarser lithologies. In LC1, mudstones deformed by bulk flexural flow, with coeval flexural slip occurring on discrete, widely spaced sheeted vein complexes. In LC2, coarser lithologies folded by orthogonal flexure, while mudstones folded by bulk flexural flow. In LC3, where the mudstones and arkoses are interbedded, orthogonal flexure occurred in the arkoses, flexural flow occurred in mudstones, and flexural slip occurred along the boundaries of coarse beds and SVCs. The presence of early cross-fold veins and the general lack of hinge-parallel fractures in all units is interpreted as evidence for early layer-parallel shortening prior to folding.

The sequence and distribution of deformation in the Taraises Formation indicates that unit T2 deformed by flexural flow, with flexural slip occurring on widely-spaced bedding-parallel veins. Flexural flow occurred in T1 to a much less significant degree and was probably accompanied by orthogonal flexure. Flexural slip along the margins of T1 likely accommodated the resulting strain incompatibility between it and adjacent rocks. Late stage tightening was accommodated by bulk shortening and limb thinning, as represented by the crenulation cleavage. This interpretation is supported by the presence of similarly oriented crenulation cleavage in the southern limb of the Muertos anticline.

Deformation in mechanical units of the Cupido Formation suggests that this interval deformed by a combination of flexural flow and slip. Early cross-fold veins, and the alignment of compaction stylolite teeth with cleavage is taken as evidence of layer-parallel shortening. Cleavage in units C1 and C2, most of which exhibit slightly different orientations in neighboring units of differing lithology, indicate that these units deformed by flexural flow. The lack of prominent cleavage, bedding-parallel, or early cross-fold veins in C3 suggests that this unit likely deformed by orthogonal flexure with significant LPS prior to folding. Unit C4 folded by a combination of flexural slip and flow, with slip occurring along bedding-parallel veins in orange–tan facies with S–C style foliations. Layers adjacent to the orange–tan horizons underwent limited flexural flow whereas units further away deformed by orthogonal flexure.

The La Peña and Aurora formations folded by a combination of flexural flow and slip, although on drastically different scales. Shaley sections and individual limestone beds of the La Peña Formation deformed by flow, with slip along the margins of the carbonate beds. Although this unit displays mesoscopic inhomogeneous deformation throughout, it is best described as deforming by homogeneous flexural flow on the scale of the Nuncios fold. The Aurora Formation accommodated folding by flexural slip on zones of stylolitic breccia and bedding-parallel veins. Where these zones are widely spaced, rocks between them deformed by flexural flow, whereas rocks between more closely spaced slip zones deformed by orthogonal flexure.

7.3. Predicted deformation patterns in Monterrey salient folds

By merging our interpreted folding mechanisms for each mechanical unit with the theoretical folding strains shown in Fig. 12, we can make general predic-

tions about deformation patterns in folds throughout the Monterrey salient. Though derived from one canyon in the frontal fold of the SMO, these predictions may be applicable to other detachment folds involving similar stratigraphy, and forming under similar environmental conditions (e.g. deep water Gulf of Mexico).

The following units folded primarily by orthogonal flexure: Zuloaga Formation, coarse layers in units LC2 and LC3, unit T1, unit C3, and Aurora Formation intervals between moderate- to closely-spaced slip surfaces. In these units, early layer-parallel shortening should suppress hinge-parallel fractures, and produce prominent cross-fold fractures in fold limbs. Any hinge-parallel fractures will be severely restricted to the structurally highest and tightest portions of folds, whereas cross-strike fractures will be widespread throughout fold limbs, less prominent in fold hinge zones, and better developed in stratigraphically higher units. Cleavage will be absent throughout these units, but bedding-parallel slip horizons may be well-developed along the boundaries of units in fold limbs. For well-bedded units with abrupt bedding interfaces, expect closely-spaced bedding-parallel slip zones.

The following units folded by flexural flow: mudstones in all units of the La Casita Formation, unit T2 in the Taraises Formation, and units C1 and C2 of the Cupido Formation. In fold limbs, these units should contain prominent cleavage whose intensity will be greater, and intersection angle with bedding will be smaller for more clay-rich intervals. Cross-fold fractures should be present in fold limbs and hinges. In the La Casita and Taraises formations these fractures should be well-developed, and the fracture network will have a geometry characteristic of systems forming in massive, homogeneous rocks (e.g. Engelder et al., 1993). Cross-fold fractures in the carbonate units will probably be confined to dolomitic intervals, and will consequently have regular spacings and restricted heights.

Late-stage tightening to interlimb angles smaller than 60° should cause additional deformation that will overprint these deformation patterns in several ways. For units folded by orthogonal flexure, bulk shortening may intensify hinge-parallel fracturing at points of high curvature, but will probably not expand the areal distribution of these fractures. Tightening of units folded by flexural flow should intensify old or create new cleavage in the fold limbs, and will thicken and create new cleavage in fold hinges. Hinge-parallel extension coeval with tightening will intensify cross-fold fractures in all units, regardless of folding mechanism, while coincidental shear along existing cross-fold fractures may cause secondary fractures to propagate and connect between them. Faults with displacements of 20–200 m may cut through all units near points of high curvature.

8. Conclusions

Deformation patterns are described by the style, intensity and distribution of structures throughout a volume of rock. Although many theoretical and field studies suggest stratigraphic parameters play a role in folding, most models of fault-related folding do not rigorously incorporate any potential stratigraphic influences on fold-related deformation patterns. One way to include such stratigraphic influences is to develop a mechanical stratigraphy that characterizes the unique deformation response of various rocks of the involved stratigraphic column.

In the forelimb of the Nuncios detachment fold of the Monterrey salient, we divided the carbonate and siliciclastic section into 13 different mechanical units. Deformation patterns in these units indicate that flexural flow, flexural slip and orthogonal flexure mechanisms were coevally or sequentially operative in various parts of the stratigraphic section. We take these folding mechanisms as the characteristic behavior of each mechanical unit, and qualitatively predict general deformation patterns in the hinges and limbs of folds with similar geometries and kinematic histories. This approach to predicting deformation patterns may be applicable to other classes of fault-related folds.

Because mechanical units in the same structure can fold by different mechanisms, we must resist the temptation to describe only the kinematic behavior of a 100 or 500 m thick sequence of competent and incompetent rocks. This simplification overlooks possible variations in strain and deformation patterns that may occur in different mechanical units, and on scales that are significant for reservoir produceability. Ultimately, we assert that the role of stratigraphic factors is equally as significant as the role of structural factors in controlling deformation patterns in fault-related folds. Although rigorously constrained sequential restorations may reveal fold kinematics, stratigraphic factors can determine the style, intensity and distribution of deformation at scales ranging from centimeters to decameters. This makes characterization of stratigraphic influences extremely important for accurate predictions of reservoir potential.

their contributions to these ideas, and are very grateful for their continuing collaboration. Mike Gross assisted us in the field for a portion of this study and suggested ways to record and present the mechanical stratigraphy. Richard Lisle and an anonymous reviewer provided helpful comments for which we are grateful. A portion of this work was completed as PBJ's MS thesis at NIU. This project was supported by a grant to MPF from the NIU Graduate Committee on Research and Artistry.

References

Anastasio, D.J., Fisher, D.M., Messina, T.A., Holl, J.E., 1997. Kinematics of décollement folding in the Lost River Range, Idaho. Journal of Structural Geology 19, 355–368.

Apotria, T.G., Wilkerson, M.S., Knewtson, S.L., 1996. 3D geometry and controls on fracturing in a natural fault-bend fold; Rosario Field, Maracaibo Basin, Venezuela. American Association of Petroleum Geologists Bulletin 80, 1268.

Bamford, M.L.F., Ford, M., 1990. Flexural shear in a periclinal fold from the Irish Variscides. Journal of Structural Geology 12, 59–67.

Barrier, J., 1977. Study of the coccoliths and Nannoconus from the Taraises; Cupido shelf margin, northern Mexico. In: Bebout, D.B., Loucks, R.G. (Eds.), Cretaceous Carbonates of Texas and Mexico; Applications to Subsurface Exploration. University of Texas Bureau of Economic Geology, pp. 295–298 (Report of Investigations 89).

Bhattacharya, A.R., 1992. A quantitative study of hinge thickness of natural folds; some implications for fold development. Tectonophysics 212, 371–377.

Behzadi, H., Dubey, A.K., 1980. Variation of interlayer slip in space and time during flexural folding. Journal of Structural Geology 2, 453–457.

Biot, M.A., 1961. Theory of folding of stratified viscoelastic media and its implications in tectonics and orogenesis. Geological Society of America Bulletin 72, 1595–1620.

Biot, M.A., 1965. Theory of internal buckling of a confined multi-layer sequence. Geological Society of America Bulletin 75, 563–568.

Bishop, B.A., 1972. Petrography and origin of Cretaceous limestones, Sierra de Picachos and vicinity, Nuevo Leon, Mexico. Journal of Sedimentary Petrology 42, 270–286.

Blauser, W.H., 1979. Geology of the southern Sierra de Catorce and stratigraphy of the Taraises Formation in north central Mexico. Unpublished MS thesis, University of Texas at Arlington, Arlington.

Cacas, M.C., Letouzey, J., Badsi, M., 1996. Application of an integrated technique for analysing naturally fractured reservoirs. American Association of Petroleum Geologists Bulletin 80, 1278.

Cantu-Chapa, A., 1989. La Pena Formation (Aptian); a condensed limestone–shale sequence from the subsurface of NE Mexico. Journal of Petroleum Geology 12, 69–83.

Carrillo-Martinez, M., 1989. Structural analysis of two juxtaposed Jurassic lithostratigraphic assemblages in the Sierra Madre Oriental fold and thrust belt of central Mexico. In: Urrutia-Fucugauchi, J. (Ed.), Dynamics and Evolution of the Lithosphere; Results and Perspectives of Earth Sciences Research in Mexico, Vol. 28. Geofisica Internacional, pp. 1007–1028.

Chapple, W.M., Spang, J.H., 1974. Significance of layer-parallel slip during folding of layered sedimentary rocks. Geological Society of America Bulletin 85, 1523–1534.

Clowes, D.M., 1990. Stratigraphy and microfacies of Canon de la Casita, Coahuila, Mexico. Unpublished MS thesis, University of Texas at Dallas, Richardson.

Conklin, J., Moore, C., 1977. Environmental analysis of the Lower Cretaceous Cupido Formation, northeast Mexico. In: Bebout, D.B., Loucks, R.G. (Eds.), Cretaceous Carbonates of Texas and Mexico; Applications to Subsurface Exploration. University of Texas Bureau of Economic Geology, pp. 302–323 (Report of Investigations 89).

Cooke, M.L., Pollard, D.D., 1997. Bedding plane slip in initial stages of fault-related folding. Journal of Structural Geology 19, 567–581.

Corbett, K., Friedman, M., Spang, J., 1987. Fracture development and mechanical stratigraphy of Austin Chalk, Texas. American Association of Petroleum Geologists Bulletin 71, 17–28.

Currie, J.B., Patnode, H.W., Trump, R.P., 1962. Development of folds in sedimentary strata. Geological Society of America Bulletin 73, 655–674.

Dahlstrom, C.D.A., 1969. Balanced cross sections. Canadian Journal of Earth Sciences 6, 743–757.

de Cserna, Z., 1956. Tectonica de la Sierra Madre Oriental de Mexico, entre Toreon y Monterrey. 20th International Geological Congress.

Dillman, G., 1985. Structural investigation and tectonic history of central Parras Basin, Saltillo, Coahuila, Mexico. Unpublished MS thesis, University of Houston, Houston, Texas.

Donath, F.A., Parker, R.B., 1964. Folds and folding. Geological Society of America Bulletin 75, 45–62.

Dubey, A.K., 1980. Late stages in the development of folds as deduced from model experiments. Tectonophysics 65, 311–322.

Elliott, D., 1983. The construction of balanced cross-sections. Journal of Structural Geology 5, 101.

Engelder, T., Fischer, M.P., Gross, M.R., 1993. Geological Aspects of Fracture Mechanics. Geological Society of America Short Course Notes.

Engelder, T., Gross, M.R., Pinkerton, P., 1997. Joint development in clastic rocks of the Elk Basin anticline, Montana–Wyoming: An analysis of fracture spacing versus bed thickness in a basement-involved Laramide structure. In: Hoak, T., Klawitter, A., Blomquist, P. (Eds.), Fractured Reservoirs: Characterization and Modeling Rocky Mountain. Association of Geologists, Denver, Colorado, pp. 1–18.

Epard, J.-L., Groshong, R.H., 1995. Kinematic model of detachment folding including limb rotation, fixed hinges and layer-parallel strain. Tectonophysics 247, 85–103.

Erslev, E.A., 1991. Trishear fault-propagation folding. Geology 19, 617–620.

Finneran, J., 1986. Carbonate petrography and depositional environments of the Upper Jurassic Zuloaga Formation, Sierra de Enfrente, Coahuila Mexico. Unpublished MS thesis, Stephen F. Austin State University, Texas.

Fischer, M.P., Woodward, N.B., 1992. The geometric evolution of foreland thrust systems. In: McClay, K.R (Ed.), Thrust Tectonics. Chapman & Hall, London.

Fischer, M.P., Woodward, N.B., Mitchell, M.M., 1992. The kinematics of break-thrust folds. Journal of Structural Geology 14, 451–460.

Fischer, M.P., Jackson, P.B., Gross, M.R., 1996. Structural geometry, fabrics and kinematics in a map-scale detachment fold: Sierra Madre Oriental, Saltillo, Mexico. Geological Society of America, Abstracts with Programs 28, A–242.

Fisher, D.M., Anastasio, D.J., 1994. Kinematic analysis of a large-scale leading-edge fold, Lost River Range, Idaho. Journal of Structural Geology 16, 337–354.

Ford, M., Williams, E.A., Artoni, A., Vergés, J., Hardy, S., 1997. Progressive evolution of a fault-related fold pair from growth

strata geometries, Sant Llorenç de Morunys, SE Pyrenees. Journal of Structural Geology 19, 413–441.

Fortunato, K.S., Ward, W.C., 1982. Upper Jurassic–Lower Cretaceous fan-delta complex, La Casita Formation of the Saltillo area, Coahuila, Mexico. Gulf Coast Association of Geological Societies Transactions 32, 473–482.

Gibbs, A.D., Jaffri, F., Murray, T., 1997. New techniques for fracture distribution and prediction from kinematic modelling of 3D strain fields. American Association of Petroleum Geologists and Society of Economic Paleontologists and Mineralogists Annual Meeting Abstracts 6, p. 40.

Goldhammer, R.G., Lehman, P.J., Todd, R.G., Wilson, J.L., Ward, W.C., Johnson, C.R., 1991. Sequence stratigraphy and cyclostratigraphy of the Mesozoic of the Sierra Madre Oriental, northeast Mexico, A Field Guidebook. Gulf Coast Section, Society of Economic Paleontologists and Mineralogists.

Gray, G.G., Johnson, C.A., 1995. Structural and tectonic evolution of the Sierra Madre Oriental, with emphasis on the Saltillo–Monterrey corridor. Guidebook for Fieldtrip No. 10, American Association of Petroleum Geologists Annual Convention.

Gross, M.R., 1995. Fracture partitioning: Failure mode as a function of lithology in the Monterey Formation of coastal California. Geological Society of American Bulletin 107, 779–792.

Gross, M.R., Engelder, T., 1995. Strain accommodated by brittle failure in adjacent units of the Monterey Formation, U.S.A.: scale effects and evidence for uniform displacement boundary conditions. Journal of Structural Geology 17, 1303–1318.

Gross, M.R., Bahat, D., Becker, A., 1997a. Relations between jointing and faulting based on fracture-spacing ratios and fault-slip profiles: A new method to estimate strain in layered rocks. Geology 25, 887–890.

Gross, M.R., Becker, A., Gutiérrez-Alonso, G., 1997b. Transfer of displacement from multiple slip zones to a major detachment in an extensional regime: Example from the Dead Sea rift, Israel. Geological Society of America Bulletin 109, 1021–1035.

Gross, M.R., Gutiérrez-Alonso, G., Bai, T., Wacker, M.A., Collinsworth, K.B., Behl, R.J., 1997c. Influence of mechanical stratigraphy and kinematics on fault scaling relations. Journal of Structural Geology 19, 171–183.

Hanks, C.L., Lorenz, J., Teufel, L., Krumhardt, A.P., 1997. Lithologic and structural controls on natural fracture distribution and behavior within the Lisburne Group, northeastern Brooks Range and North Slope subsurface, Alaska. American Association of Petroleum Geologists Bulletin 81, 1700–1720.

Hardy, S., Ford, M., 1997. Numerical modeling of trishear fault propagation folding. Tectonics 16, 841–854.

Hennings, P.H., Olson, J.E., 1997. The relationship between bed curvature and fracture occurrence in a fault-propagation fold. American Association of Petroleum Geologists and Society of Economic Paleontologists and Mineralogists Annual Meeting Abstracts 6, p. 49.

Homza, T.X., Wallace, W.K., 1995. Geometric and kinematic models for detachment folds with fixed and variable detachment depths. Journal of Structural Geology 17, 575–588.

Homza, T.X., Wallace, W.K., 1997. Detachment folds with fixed hinges and variable detachment depth, northeastern Brooks Range, Alaska. Journal of Structural Geology 19, 337–354.

Hudleston, P.J., 1973. Fold morphology and some geometrical implications of theories of fold development. Tectonophysics 16, 1–46.

Hudleston, P.J., Holst, T.B., 1984. Strain analysis and fold shape in a limestone layer and implications for layer rheology. Tectonophysics 106, 321–347.

Hudleston, P.J., Lan, L., 1994. Rheological controls on the shapes of single-layer folds. Journal of Structural Geology 16, 1007–1021.

Hudleston, P.J., Treagus, S.H., Labao, L., 1996. Flexural flow folding: does it occur in nature? Geology 24, 203–206.

Humphrey, W.E., 1949. Geology of the Sierra de los Muertos area, Mexico. Geological Society of America Bulletin 60, 89–176.

Humphrey, W.E., 1954. Stratigraphy of the Cortinas Canyon section, Sierra de los Muertos, Coahuila, Mexico. South Texas Geological Society Guidebook, 21st Field Trip.

Jamison, W.R., 1987. Geometric analysis of fold development in overthrust terranes. Journal of Structural Geology 9, 207–219.

Jamison, W.R., 1992. Stress controls on fold thrust style. In: McClay, K.R (Ed.), Thrust Tectonics. Chapman & Hall, London, pp. 155–164.

Johnson, A.M., 1977. Styles of Folding. Elsevier, New York.

Johnson, C.A., Gray, G.G., Goldhammer, R.K., 1991. Structure and tectonics of the Sierra Madre Oriental fold–thrust belt near Monterrey, northeastern Mexico. American Association of Petroleum Geologists Bulletin 75, 603.

Johnson, C.R., 1991. Depositional cycles of the Zuloaga (Oxfordian–Kimmeridgian?) Formation, Sierra de Bunuelos, Coahuila, Mexico. Unpublished MS thesis, University of New Orleans, New Orleans, Louisiana.

Kindred, F.R., 1988. Origin and diagenesis of carbonate mudstone, shallow to deeper shelf, Aurora Formation, Coahuila, Mexico. Unpublished MS thesis, University of New Orleans, New Orleans, Louisiana.

Laudon, R.C., 1984. Evaporite diapirs in the La Popa Basin, Nuevo Leon, Mexico. Geological Society of America Bulletin 95, 1219–1225.

Lemiszki, P.J., Landes, J.D., Hatcher Jr, R.D., 1994. Controls on hinge-parallel extension fracturing in single-layer tangential longitudinal strain folds. Journal of Geophysical Research 99, 22027–22041.

Lickorish, W.H., Butler, R.W.H., 1996. Fold amplification and parasequence stacking patterns in syntectonic shoreface carbonates. Geological Society of America Bulletin 108, 966–977.

Lisle, R.J., 1994. Detection of zones of abnormal strains in structures using Gaussian curvature analysis. American Association of Petroleum Geologists Bulletin 78, 1811–1819.

Lister, G.S., Snoke, A.W., 1984. *S–C* mylonites. Journal of Structural Geology 6, 617–638.

Lozej, G.P., Beales, F., 1977. Stratigraphy and structure of La Encantada Mine area, Coahuila, Mexico. Geological Society of America Bulletin 88, 1793–1807.

McBride, E.F., Weidie, A.E., Wollenben, J.A., Laudon, R.C., 1974. Stratigraphy and structure of the Parras and La Popa Basin, northeastern Mexico. Geological Society of America Bulletin 85, 1603–1622.

Meyer, M.G., Ward, W.C., 1984. Outer-ramp limestones of the Zuloaga Formation, Astillero Canyon, Zacatecas, Mexico. In: Ventress, W.P.S., et al. (Eds.), The Jurassic of the Gulf Rim. Gulf Coast Section Society of Economic Paleontologists and Mineralogists, Proceedings of the Third Annual Research Conference, pp. 275–282.

Mitchell, M.M., Woodward, N.B., 1988. Kink detachment fold in the southwest Montana fold and thrust belt. Geology 16, 162–165.

Mitre-Salazar, L.M., 1981. Las imagenes Landsat; una herramienta util en la interpretacion geologico-estructural; un ejemplo en el noreste de Mexico (Translated title: Landsat imagery; a useful tool in geological–structural interpretation; an example from northeastern Mexico). Revista Instituto de Geologia 5, 37–46.

Ovianki, S.M., 1974. Paleodepositional environments in the Upper Jurassic Zuloaga Formation (Smackover), northeast Mexico. Gulf Coast Association of Geological Societies Transactions 24, 258–278.

Padilla y Sanchez, R., 1982. Geologic evolution of the Sierra Madre Oriental between Linares, concepcion del Oro, Saltillo, and Monterrey, Mexico. Unpublished PhD thesis, University of Texas at Austin, Austin, Texas.

Piaggio, A.D., 1961. The Los Nogales Member of the Taraises Formation (Lower Cretaceous) near Monterrey, Nuevo Leon, Mexico. Unpublished MS thesis, Tulane University, New Orleans, Louisiana.

Quintero-Legorreta, O., Aranda-Garcia, M., 1985. Relaciones estructurales entre el Anticlinorio de Parras y el Anticlinorio de Arteaga (Sierra Madre Oriental), en la region de Agua Nueva, Coahuila (Translated title: Structural relations in the Parras and Arteaga anticlinoria (Sierra Madre Oriental), in the region of Agua Nueva Coahuila). Revista Instituto de Geologia 6, 21–36.

Ramberg, H., 1961. Relationship between concentric longitudinal strain and concentric shearing strain during folding of homogeneous sheets of rock. American Journal of Science 259, 382–390.

Ramberg, H., 1963. Strain distribution and geometry of folds. Bulletin of the Geological Institute of the University of Uppsala 42, 1–20.

Ramberg, H., 1964. Selective buckling of composite layers with contrasted rheological properties. A theory for simultaneous formation of several orders of folds. Tectonophysics 1, 307–341.

Ramsay, J.G., 1967. Folding and Fracturing of Rocks. McGraw-Hill, New York.

Ramsay, J.G, Huber, M.I., 1987a. In: Strain Analysis, The Techniques of Modern Structural Geology, Vol. 1. Academic Press, London.

Ramsay, J.G., Huber, M.I., 1987b. In: Folds and Fractures, The Techniques of Modern Structural Geology, Vol. 2. Academic Press, London.

Rowan, M.G., Kligfield, R., 1992. Kinematics of large-scale asymmetric buckle folds in overthrust shear: an example from the Helvetic nappes. In: McClay, K.R (Ed.), Thrust Tectonics. Chapman & Hall, London, pp. 165–173.

Salvini, F., Storti, F., 1997. Spatial and temporal distribution of fractured rock panels from geometric and kinematic models of thrust-related folding. American Association of Petroleum Geologists Bulletin 81, 1409.

Selvius, D.B., 1982. Lithostratigraphy and algal-foraminiferal biostratigraphy of the Cupido Formation, Lower Cretaceous, in Bustamante Canyon and Potrero Garcia, northeast Mexico. Unpublished MS thesis, The University of Michigan, Ann Arbor, Michigan.

Smith, C.R., 1987. Provenance and depositional environments of the La Casita Formation, Sierra Madre Oriental, southwest of Monterrey, northeastern Mexico. Unpublished MS thesis, University of New Orleans, New Orleans, Louisiana.

Spang, J.H., McConnell, D.A., 1997. Effect of initial fault geometry on the development of fixed-hinge, fault-propagation folds. Journal of Structural Geology 19, 1537–1541.

Stabler, C.L., Marquez, B., 1977. Initiation of Lower Cretaceous reefs in Sabinas basin, northeast Mexico. In: Bebout, D.G., Loucks, R.G. (Eds.), Cretaceous Carbonates of Texas and Mexico; Applications to Subsurface Exploration. University of Texas Bureau of Economic Geology, pp. 299–301 (Report of Investigations 89).

Suppe, J., 1983. Geometry and kinematics of fault-bend folding. American Journal of Science 283, 684–721.

Suppe, J., Medwedeff, D.A., 1984. Fault-propagation folding. Geological Society of America, Abstracts with Programs 16, 670.

Suppe, J., Medwedeff, D.A., 1990. Geometry and kinematics of fault-propagation folding. Eclogae Geologica Helvetiae 83, 409–454.

Suppe, J., Sabat, F., Muñoz, J.A., Poblet, J., Roca, E., Vergés, J., 1997. Bed-by-bed fold growth by kink-band migration: Sant Llorenç de Morunys, eastern Pyrenees. Journal of Structural Geology 19, 443–461.

Suter, M., 1987. Structural traverse across the Sierra Madre Oriental fold–thrust belt in east-central Mexico. Geological Society of America Bulletin 98, 249–264.

Tanner, P.W.G., 1989. The flexural slip mechanism. Journal of Structural Geology 11, 635–655.

Tanner, P.W.G., 1992. Morphology and geometry of duplexes formed during flexural-slip folding. Journal of Structural Geology 14, 1173–1192.

Taylor, E.P., 1993. The structural geology of La Popa Basin, Nuevo Leon, Mexico. Unpublished MS thesis, University of New Orleans, New Orleans, Louisiana.

Thorbjornsen, K.L., Dunne, W.M., 1997. Origin of a thrust-related fold: geometric vs kinematic tests. Journal of Structural Geology 19, 303–319.

Tinker, S.W., 1982. Lithostratigraphy and biostratigraphy of the Aptian La Pena Formation, northeast Mexico and South Texas (Part 1), and the depositional setting of the Aptian Pearsall–La Pena Formations, Texas subsurface and northeast Mexico: Why is there not another Fairway Field? (Part 2). Unpublished MS thesis, The University of Michigan, Ann Arbor, Michigan.

Treagus, S.H., 1988. Strain refraction in layered systems. Journal of Structural Geology 10, 517–527.

Twiss, R.J., Moores, E.M., 1992. Structural Geology. W.H. Freeman, New York.

Wall, J.R., Murray, G.E., Diaz, T., 1961. Geologic occurrence of intrusive gypsum and its effect on structural forms in Coahuila Marginal fold province of northeastern Mexico. American Association of Petroleum Geologists Bulletin 45, 1504–1522.

Weidie, A.E., Martinez, J.D., 1970. Evidence for evaporite diapirism in northeastern Mexico. American Association of Petroleum Geologists Bulletin 54, 655–661.

Weidie, A.E., Murray, G.E., 1967. Geology of the Parras Basin and adjacent areas of northeastern Mexico. American Association of Petroleum Geologists Bulletin 51, 678–695.

Wilson, J.L., 1981. Lower Cretaceous stratigraphy in the Monterrey–Saltillo area. In: Smith, C.I (Ed.), Lower Cretaceous Stratigraphy and Structure, Northern Mexico. West Texas Geological Society, pp. 78–84 (Publication 81-74).

Wilson, J.L., Pialli, G., 1977. A Lower Cretaceous shelf margin in northern Mexico. In: Bebout, D.G., Loucks, R.G. (Eds.), Cretaceous Carbonates of Texas and Mexico; Applications to Subsurface Exploration. University of Texas Bureau of Economic Geology, pp. 286–294 (Report of Investigations 89).

Wilson, J.L., Selvius, D.B., 1984. Early Cretaceous in the Monterrey–Saltillo area of northern Mexico. In: Wilson, J.L., Ward, W.C., Finneran, J. (Eds.), A Field Guide to Upper Jurassic and Lower Cretaceous Carbonate Platform and Basin Systems, Monterrey–Saltillo Area, Northeast Mexico. Gulf Coast Section. Society of Economic Paleontologists and Mineralogists, pp. 28–42.

Wilson, J.L., Ward, W.C., 1993. Early Cretaceous carbonate platforms of northeastern and east-central Mexico. In: Simo, J.A.T., Scott, R.W., Masse, J.-P. (Eds.), Cretaceous Carbonate Platforms. American Association of Petroleum Geologists Memoir 56, pp. 35–49.

Williams, E., 1966. An analysis of the deformation in a fold in north-east Tasmania. Geological Magazine 103, 115–119.

Wojtal, S.F., 1989. Measuring displacement gradients and strains in faulted rocks. Journal of Structural Geology 11, 669–678.

Woodward, N.B., Boyer, S.E., Suppe, J., 1985. An Outline of Balanced Cross Sections. University of Tennessee Department of Geological Sciences Studies in Geology 11.